Received: 27 July 2021 | Revised: 10 November 2021 | Accepted: 13 November 2021
DOI: 10.1002/jmor.21431

RESEARCH ARTICLE

JOURNAL OF morphology WILEY

The morphology of the suboccipital region in snakes, and the anatomical and functional diversity of the myodural bridge

Bryson Grondel | Michael Cramberg | Skye Greer | Bruce A. Young

Department of Anatomy, Kirksville College of Osteopathic Medicine, Kirksville, Missouri, USA

Correspondence
Bruce A. Young, Department of Anatomy, Kirksville College of Osteopathic Medicine, Kirksville, MO 63501, USA.
Email: byoung@atsu.edu

Funding information
A portion of this project was funded through an internal (Warner/Fermaturo) grant to Bruce A. Young.

Abstract

The myodural bridge, that is, skeletal muscle fibers attaching to the cervical dura mater, has been described from a variety of mammals and other amniotes. To test an earlier assumption about the presence of the myodural bridge in snakes, a comparative study was designed using a group of Colubrine snakes. Serial histological sections revealed no evidence of the myodural bridge in any of the snakes examined. Further analyses, including histology, computed tomography (CT), and micro-CT imaging of other distantly related snakes, also turned up no evidence of a myodural bridge. The close apposition of adjacent neural arches in snakes may preclude muscle tendons from passing through the intervertebral joint to reach the spinal dura. It is hypothesized that the myodural bridge functions in the clearance of the cerebrospinal fluid (CSF) by creating episodic CSF pressure pulsations, and that snakes are capable of creating equivalent CSF pressure pulsations through vertebral displacement.

KEYWORDS
cerebrospinal fluid, cervical, intervertebral, musculoskeletal, reptilia

1 | INTRODUCTION

A recent contribution (Young, Greer, & Cramberg, 2021) reported that propagating waves of vertebral displacement, as happens during feigned and natural locomotion in snakes, resulted in corresponding waves of pressure change within the cerebrospinal fluid (CSF). The motive force for the change in CSF pressure was postulated to be one of, or a combination of, three influences: change in momentum (impulse) acting on the CSF, lateral displacement of the spinal cord within the vertebral canal, or displacement of the spinal dura (Young, Greer, & Cramberg, 2021). Dural displacement is the most investigated of these three possible influences, due to the increased attention to the "myodural bridge" or MDB.

As originally described (Hack et al., 1995), the MDB consists of deep fibers of the rectus capitis posterior minor muscle which course between the occipital bone and the atlas, pass through the posterior atlantooccipital membrane, and insert, through separate tendinous slips, onto the spinal dura mater (Enix et al., 2014; Palomeque-del-Cerro et al., 2017). Venne et al. (2017) performed a biomechanical analysis of human cadaveric MDB and demonstrated that tensile force applied to the muscle resulted in significant displacement of the spinal dura. Subsequent experiments with live alligators (Young, Adams, et al., 2021; Young et al., 2020) and dogs (Ma et al., 2021) demonstrated that electrical stimulation of the musculature of the MDB resulted in significant changes to CSF pressure.

Comparative studies have described an MDB in a variety of terrestrial mammals (e.g., Elbrond & Schultz, 2019; Lai et al., 2020; Zhang et al., 2020; Zheng et al., 2017) as well as three species of cetacean (Liu et al., 2017, 2018; Zheng et al., 2017). The number of mammalian taxa examined led Zheng et al. (2017) to argue that the MDB was a consistent feature among mammals. An MDB has also been reported in several bird species (Chen et al., 2021; Dou et al., 2019; Okoye et al., 2018), in Crocodylians (Young et al., 2020; Zhang et al., 2016), and in the turtle *Trachemys scripta* (Huangfu et al., 2019). The diversity of taxa studied to date, combined with the absence of accounts of taxa lacking the feature, suggests that the MDB may be a common attribute of amniotes. Young, Greer, and Cramberg (2021) assumed the presence of an MDB in snakes; one of the primary purposes of the present study is to explicitly test this assumption by documenting the anatomical relationship of the suboccipital muscles and cervical spinal dura in snakes.

Influencing the spinal CSF dynamics is not the only proposed function of the MDB; it has also been interpreted as a proprioceptive structure (e.g., Hallgren et al., 1997), and as a specialization to restrict displacement and pleating of the dura (e.g., Hack et al., 1995). Evaluating the functional role, or roles, of the MDB is challenging, in part, because some authors have applied the term "myodural bridge" to anatomical complexes that lack some of the anatomical features Hack et al. (1995) associated with the MDB (see Palomeque-del-Cerro et al., 2017). Many of these MDB-like complexes rely on fascial connections, rather than muscle tendon, and the biomechanics of these fascial links have yet to be explored (e.g., Bordoni & Myers, 2021). Another primary purpose of the present study is to explore how the structure of the suboccipital region in snakes may inform the anatomical diversity and functional interpretations that have been applied to the MDB.

2 | MATERIALS AND METHODS

2.1 | Comparative sample

A comparative histological analysis was performed on the suboccipital region of juvenile to sub-adult specimens from four colubrid snake species. Four specimens of Herald snake, *Crotaphopeltis hotamboeia* (Laurenti, 1768) with snout-vent lengths of 34–43 cm, four specimens of Common egg-eating snake, *Dasypeltis scabra* (Linnaeus, 1758) with snout-vent lengths of 37–46 cm, four specimens of Spotted bush snake, *Philothamnus semivariegatus* (Smith, 1840) with snout-vent lengths of 57–77 cm, and two specimens of Blanding's tree snake, *Toxicodryas blandingii* (Hallowell, 1844) with snout-vent lengths of 152 and 173 cm) were obtained commercially.

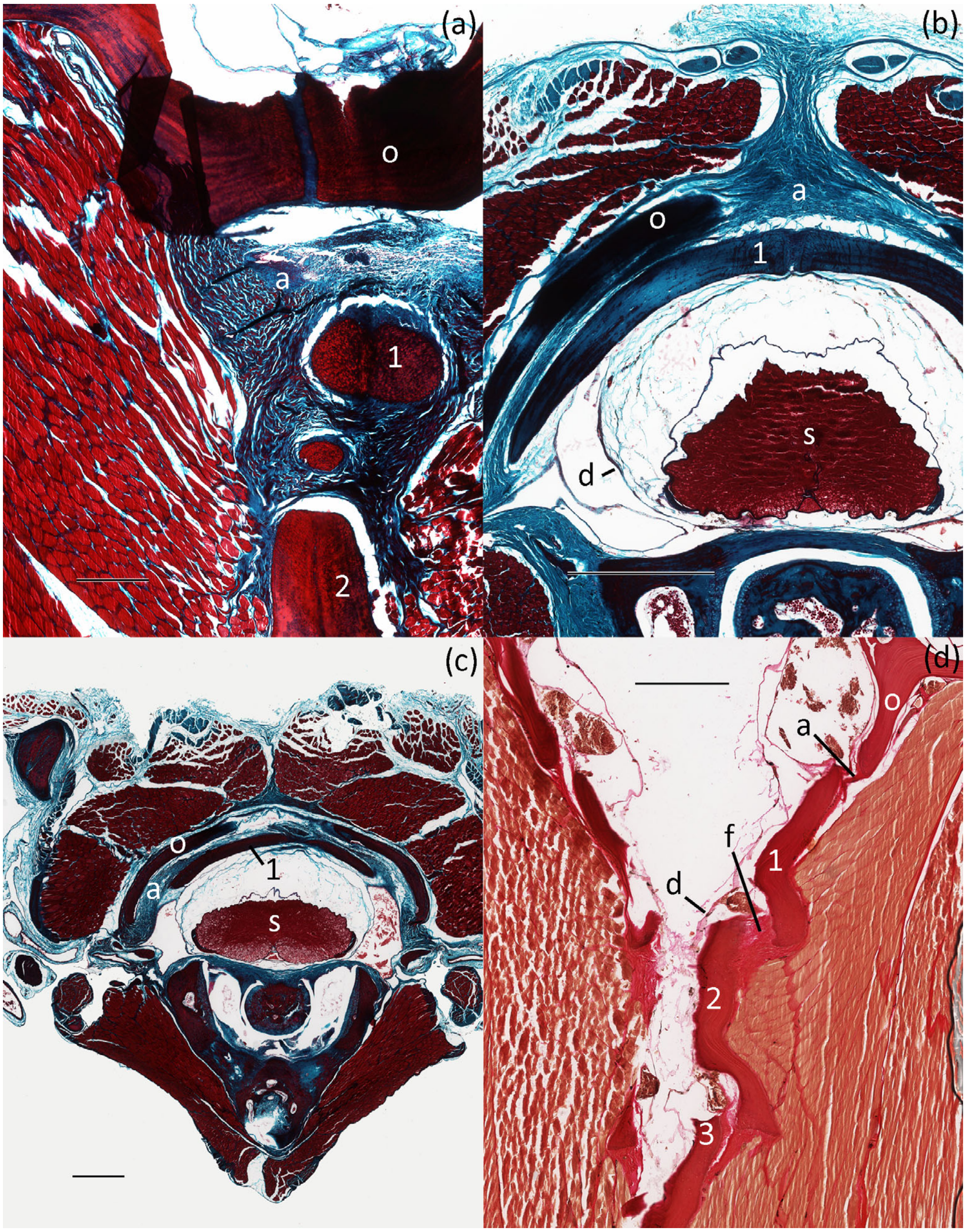

FIGURE 1 Morphology of the dorsal contact between the skull and C1 (atlas). (a) Frontal section from *Toxicodryas blandingii*. (b) Transverse section from *Dasypeltis scabra*. (c) Transverse section from *Philothamnus semivariegatus*. (d) Frontal section from *Crotaphopeltis hotamboeia*; this section was at a more ventral level (approaching the pedicle) than the one shown in (a). In all four species, the cranial surface of C1 was ventral to the caudal margin of the otoccipital, the atlantooccipital membrane was reduced, and there was no evidence for skeletal muscle fibers/fascicles diverging toward this joint. 1, C1 vertebra (atlas); 2, C2 vertebra (axis); 3, C3 vertebra; a, atlantooccipital membrane; d, dura mater; o, otoccipital; s, spinal cord. The scale bar in each image = 500 μm

The snakes were anesthetized with isoflurane then euthanized through cardiac excision and exsanguination. A peristaltic pump (Fisher) was used to flush the vascular system with heparinized reptilian Ringer's solution (Barfuss & Dantzler, 1976), then to perfuse the snake with neutral-buffered formalin. The care and use of these snakes was approved by the Institutional Animal Care and Use Committee of the Kirksville College of Osteopathic Medicine (Protocol #175, Approved 8/2016).

These four colubrid species were selected to form a natural experiment to explore some of the existing hypotheses for the function of the MDB. These snakes are from two sister clades of the Indo-African radiation of the subfamily Colubrinae (as restricted by Figueroa et al., 2016), and all four are considered active (rather than passive or ambush) foragers (e.g., Glaudas et al., 2019). *C. hotamboeia* and *D. scabra* are predominantly terrestrial species, while *P. semivariegatus* and *T. blandingii* are strongly arboreal (e.g., Broadley, 1983; Spawls & Branch, 1995). This ecological distinction is central to this study; a recent study (Young, Greer, & Cramberg, 2021) demonstrated that in snakes, like other reptiles (Kondrashova et al., 2020), the CSF is actively displaced and undergoes marked pressure swings in response to gravitational gradients. Accordingly, we hypothesize that if the MDB functions as a sensory system, it will be significantly more developed (either in terms of dural contact area or sense organs per volume of muscle fibers) in the two arboreal snake species than in the two terrestrial snake species. The ventilatory cycle of the snake results in a corresponding pressure cycle in the CSF (Young, Greer, & Cramberg, 2021), previous studies have shown that the ventilatory cycle drives spinal CSF flow (e.g., Dreha-Kulaczewski et al., 2015); we hypothesize that if the MDB functions to influence spinal CSF flow, it will be similar among the four colubrid snake species. Assuming that the structure of the spinal dura is similar in these phylogenetically closely related taxa, we hypothesize that if the MDB functions to support the dura around the foramen magnum, it will be similar in the four colubrid snakes examined.

2.2 | Histological preparation

The head and neck of each specimen was stored in neutral-buffered formalin for a minimum of 48 h at 4°C, then transferred to 70% ethanol. The skin was removed from each specimen before it was placed

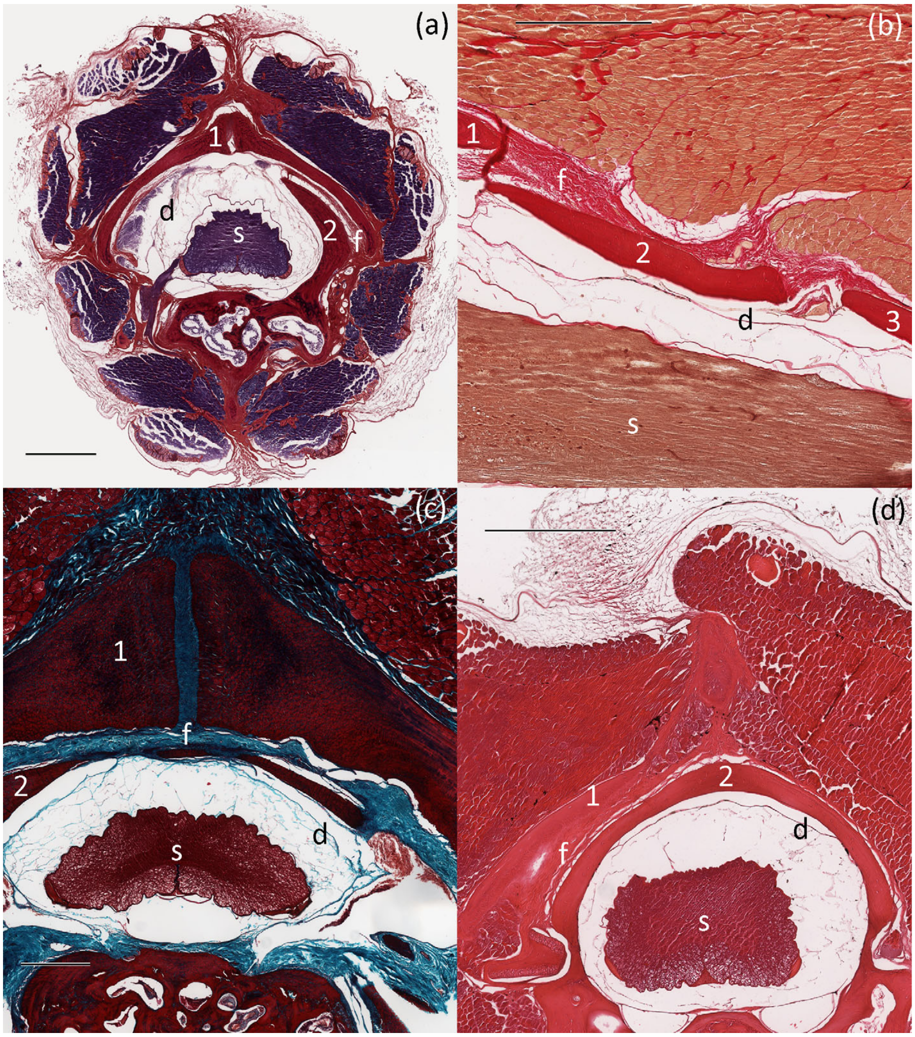

FIGURE 2 Morphology of contact between the C1/C2 neural arches. (a) Transverse section from *Dasypeltis scabra*. (b) Sagittal section from *Philothamnus semivariegatus*. (c) Transverse section from *Toxicodryas blandingii*. (d) Transverse section from *Crotaphopeltis hotamboeia*. In all four species, the cranial surface of C2 neural arch was ventral to the caudal margin of the C1 neural arch, the ligamentum flavum coursed between the two arches, and there was no evidence for skeletal muscle fibers/fascicles diverging toward this joint. 1, C1 vertebra (atlas); 2, C2 vertebra (axis); 3, C3 vertebra; d, dura mater; f, ligamentum flavum; s, spinal cord. The scale bar in each image = 500 μm

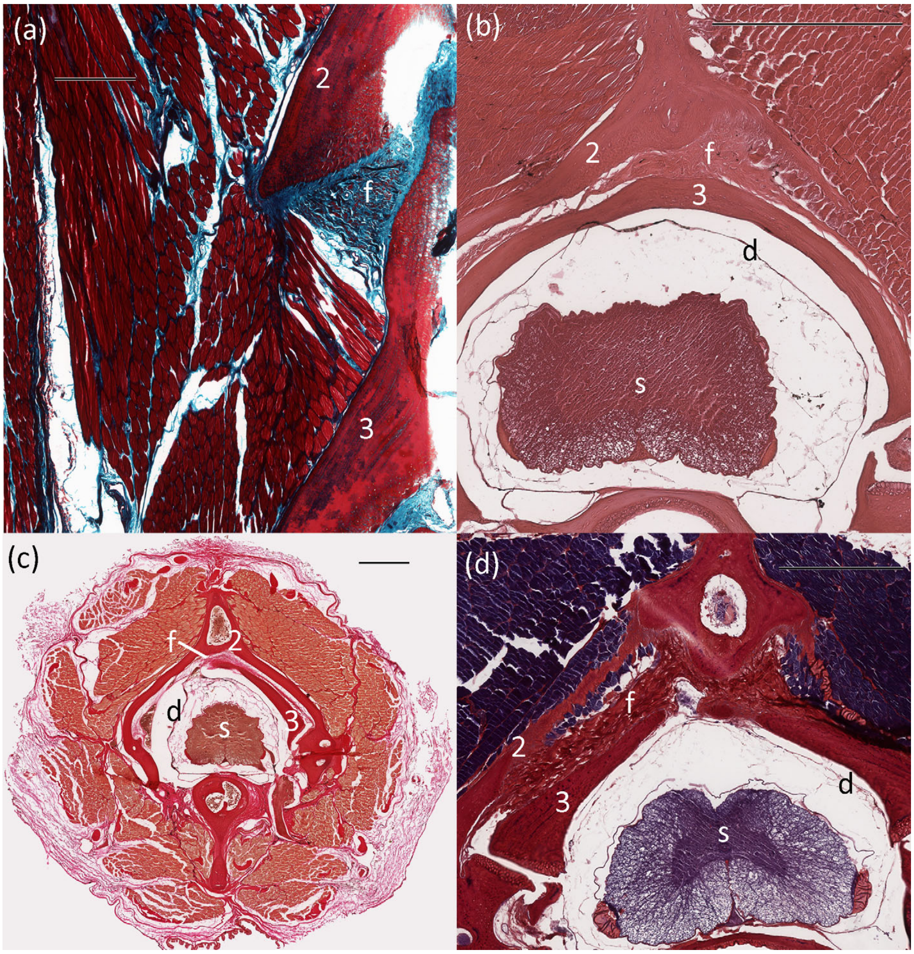

FIGURE 3 Morphology of the contact between the C2/C3 neural arches. (a) Frontal section from *Toxicodryas blandingii*. (b) Transverse section from *Crotaphopeltis hotamboeia*. (c) Transverse section from *Dasypeltis scabra*. (d) Transverse section from *Philothamnus semivariegatus*. In all four species, the cranial surface of C3 neural arch was ventral to the caudal margin of the C2 neural arch, and the ligamentum flavum coursed between the two arches. Skeletal muscle fibers/fascicles originated from the neural arch of C3 and the adjacent ligamentum flavum, but never diverged toward the C2/C3 joint. 2, C2 vertebra (axis); 3, C3 vertebra; d, dura mater; f, ligamentum flavum; s, spinal cord. The scale bar in each image = 500 μm

in RDO Rapid Decalcifier for 24–48 h, then dehydrated through an ethanol series prior to paraffin embedding. Complete serial transverse and frontal sections were cut (at 10 μm) from all four species. Additional complete serial sagittal and transverse sections were cut (at 10 μm) from *C. hotamboeia*, *D. scabra*, and *P. semivariegatus*. Sections were stained with hematoxylin and eosin, Van Gieson's/Weigert's hematoxylin stain, Masson's trichrome stain, phosphotungstic acid hematoxylin (PTAH) stain, and Picrosirius. Microscopic anatomy was documented using a DM 4000B microscope (Leica Microsystems Inc.).

2.3 | Broader analyses

To ensure that our results could be extended beyond these two Indo-African colubrid radiations, we also examined the suboccipital region of the western diamondback rattlesnake, *Crotalus atrox* (Baird and Girard, 1853), and the king cobra, *Ophiophagus hannah* (Cantor, 1836). These two snake species are only distantly related to one another, and neither are in the same phylogenetic clade as the sampled colubrid snakes (Figueroa et al., 2016). Four *C. atrox* (snout-vent lengths of 112–134 cm) were obtained commercially and prepared as detailed above. One of the *C. atrox* was pretreated in Lugol's solution then scanned at the University of Texas High-Resolution X-ray CT Facility using a custom-built North Star Imaging scanner in volume mode. The X-ray source was set to 130 kV and 0.14 mA with an aluminum foil prefilter. A total of 3600 projections were acquired over 360 degrees of rotation, at 1 frame per second with no frame averaging and no detector binning. A beam-hardening correction of 0.25 was applied; the resulting slices measured 1979 × 1979 pixels and had a voxel resolution of 9.65 μm edge length. The remaining three specimens of *C. atrox* were used for histological analyses (as described above) in the transverse and sagittal planes.

A previously preserved *O. hannah* (snout-vent length of 347 cm) from the private collection of BAY, was positioned in a clinical 64-detector CT unit (Ingenuity, Philips Medical, Einthoven, the Netherlands). Images were captured through helical acquisition at 0.67 mm, FOV 160 mm, 100 kV, 125 mAs, with a rotation time of 500 ms, section thickness of 0.67 mm, and pitch of 0.391. Images were reconstructed using the Ingenuity custom software.

As a positive control, we also examined the suboccipital anatomy of the American alligator, *Alligator mississippiensis* (Daudin, 1802), a species in which the MDB has been previously described (Young, Adams, et al., 2021; Young et al., 2020). A sub-adult *A. mississippiensis* (total length of 188 cm) was anesthetized with isoflurane then imaged using a CT unit as described above. Four hatchling *A. mississippiensis*

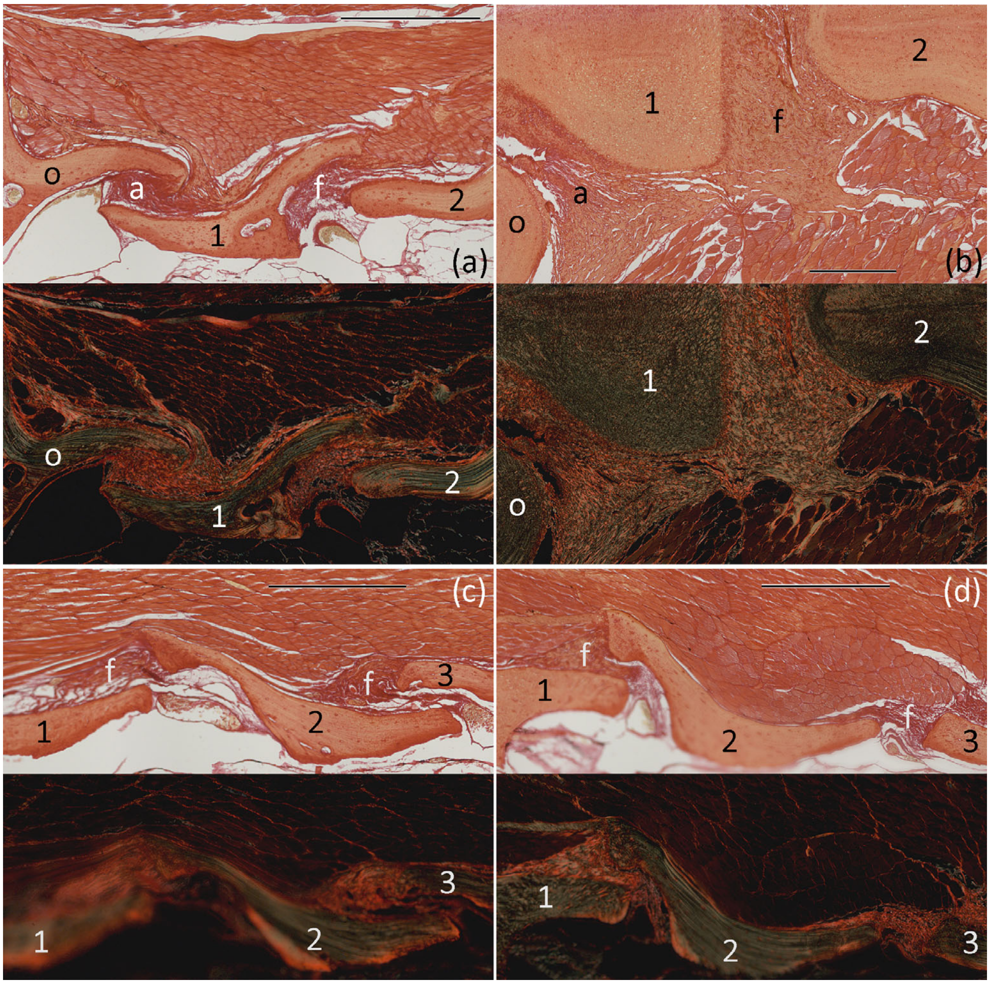

FIGURE 4 Picrosirius stained polarized microscopy of the connective tissue between the dura and the axial musculature. (a) Frontal section from *Dasypeltis scabra*. (b) Frontal section from *Toxicodryas blandingii*. (c) Sagittal section from *Philothamnus semivariegatus*. (d) Sagittal section from *Crotaphopeltis hotamboeia*. Each section is shown in brightfield (upper) for orientation, then in polarized light (lower) to emphasize the collagen fibers. In all four species, in both planes, and in all of the intervertebral joints examined, there were no collagenous elements that coursed from skeletal muscle, passing through the joint, to reach the dura. 1, C1 vertebra (atlas); 2, C2 vertebra (axis); 3, C3 vertebra; a, atlantooccipital membrane; f, ligamentum flavum; o, otoccipital; s, spinal cord. The scale bar in each image = 500 μm

(total lengths of 32–36.5 cm) were obtained commercially and euthanized as detailed above. One of the hatchling specimens was used for micro-CT analysis (as detailed above), the remaining three were used for histological analyses (as detailed above).

3 | RESULTS

3.1 | Comparative anatomy of the four colubrine snakes

At the otoccipital-atlas joint of all four colubrid species, there was a block of dense irregular connective tissue on the dorsal midline between the paired, unfused, neural arches of the atlas. This block of connective tissue is integrated into a sheet of connective tissue, herein referred to as the atlantooccipital membrane, which spans between the neural arches of C1 and the caudal surface of the otoccipital lateral and dorsal to the foramen magnum (Figure 1a). In the four colubrid species, the cranial surfaces of the C1 neural arches were covered superiorly (and laterally) by portions of the otoccipital (Figure 1b). The abutment and overlap between the caudal surface of the otoccipital and the cranial surface of the C1 neural arches was extensive enough that no transverse sections could be cut that included only the gap between these two skeletal elements; that is, a section that included the atlantooccipital membrane but neither the atlas nor otoccipital boney elements.

The sections through the colubrid species included the spinalis and, the immediately deeper, rectus capitis posterior inferior. None of these sections revealed muscle fibers or fascicles that deviated from the primary course of either muscle to approach the atlantooccipital membrane (Figure 1c). The fibers of the rectus capitis posterior inferior coursed roughly perpendicular to the atlantooccipital membrane with nothing more than a weak fascial connection between the two (Figure 1d).

At the atlanto-axial joint the cranial surface of the neural arch of C2 was ventral to the caudal surface of the neural arch of CI (Figure 2a) in all four of the colubrid species. The two neural arches were bound by dense connective tissue herein termed the ligamentum flavum. The axial muscles coursing over the C1/C2 neural arches did not include fascicles/fibers that diverged from the rest of the muscle and approached the ligamentum flavum (Figure 2c,d).

At the axis/C3 joint, the cranial surface of the fused neural arches of C3 were inferior to the caudal surface of the fused neural arches of C2 in the four colubrid species. These two neural arches were bound by the ligamentum flavum (Figure 3a,b), as well as by additional connective tissue elements that bound their respective neural spines. At

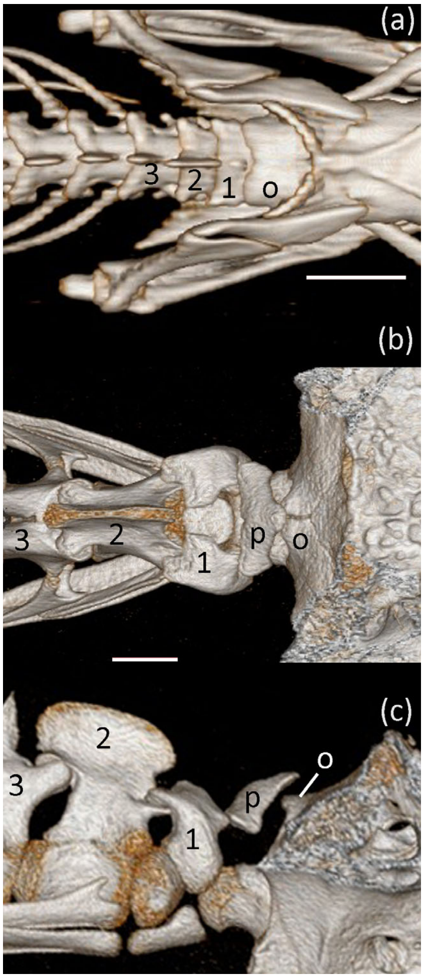

FIGURE 5 Computed tomographic (CT) reconstructions of the upper cervical vertebrae. (a) *Ophiophagus hannah* shows the close apposition of the neural arches of the ophidian cervical vertebrae. (b) Dorsal, and (c) lateral, views of *Alligator mississippiensis* showing the considerable space cranially between C1 and the skull (the caudolateral portion of the skull has been digitally removed for clarity). 1, C1 vertebra (atlas); 2, C2 vertebra (axis); 3, C3 vertebra; o, otoccipital; p, proatlas. The scale bar in each image is = 1 cm

the C2/C3 joint the rectus capitis posterior inferior has an origin from the ligamentum flavum. At this origin, there is an integration between the muscle fibers and the ligamentum flavum (Figure 3c,d), but this integration is restricted to the peripheral (lateral) portion of the ligament. In none of the four species did the muscle fibers penetrate the inner (medial) portion of the ligament.

Picrosirius staining and polarized light microscopy were used to follow the size and orientation of the collagen fibers at these three joints in the four colubrid species. At the joint between the otoccipital and neural arch of C1, no collagen fibers were found coursing from any of the suboccipital muscles, passing through the atlantooccipital membrane, and contacting the dura (Figure 4a,b). At the C1/C2 joint, there were no collagen fibers spanning from the dura, through the ligamentum flavum, to any skeletal muscle (Figure 4c,d). At the C2/C3 joint there was clear integration between fibers of the rectus capitis posterior inferior and collagen of the ligamentum flavum; but these collagen fibers did not extend medially through the ligamentum flavum to contact the dura (Figure 4d,e).

3.2 | Cervical anatomy of snakes and alligators

To extend the comparison further, representatives from two other snake families were examined, and compared to the American alligator (*A. mississippiensis*) a reptile known to have a MDB. In the king cobra (*O. hannah*) the atlas is closely abutted to the otooccipital, and the neural arches of the vertebrae show considerable overlapping (Figure 5a), the same structural pattern that was observed in the four colubrid species, and in *C. atrox*. In contrast, the neural arches of the upper cervical vertebrae of *A. mississippiensis* are spatially separated (Figure 5b,c). There is a separate proatlas bone that is invested in the atlantooccipital membrane, but does not articulate with either the caudal surface of the skull or the cranial surface of C1. There is also a distinct gap between the neural arches of C1 and C2 (Figure 5b,c).

In *C. atrox*, as with the other snake species examined, there were no clear specialized groups of muscle fibers or fascicles, which diverged from any of the axial muscles to interact with the dura (Figure 6a,c). In *A. mississippiensis* a portion of the rectus capitis posterior inferior deviates medially to integrate with the connective tissue on the cranial and caudal sides of the proatlas. In both histological and micro-CT sections of *A. mississippiensis* there is continuous connective tissue linking these muscle fibers and the dura (Figure 6b,d). Sagittal sections through *A. mississippiensis* clearly demonstrate tendon-like connective tissue elements passing around the proatlas to attach to the outer surface of the dura (Figure 6e), no similar structures were observed in any of the snake species examined.

4 | DISCUSSION

This project was designed to test for differences in the MDB among four closely related, but ecologically diverse, colubrine snakes. Our initial working definition of the MDB followed that of Hack et al. (1995) and included three specific components: (1) diverging fascicle/fibers of the rectus capitis posterior inferior; (2) tendinous slips of this muscle penetrating the atlantooccipital membrane to pass between the atlas and the skull; and (3) an attachment of these tendinous slips onto the dura. None of the three components described by Hack et al. (1995) were found in the four colubrine species (Figures 1–4). These three components were also lacking in *C. atrox* and *O. hannah*, two snake species that are only distantly related to each other and to the colubrine species examined (e.g., Wiens et al., 2012). Though we could find no evidence of an MDB in any of the snake species examined, all three components were clearly evident in *A. mississippiensis* (Figure 6) as was previously reported from this species (Young, Adams, et al., 2021; Young et al., 2020) and a related crocodilian (Zhang et al., 2016).

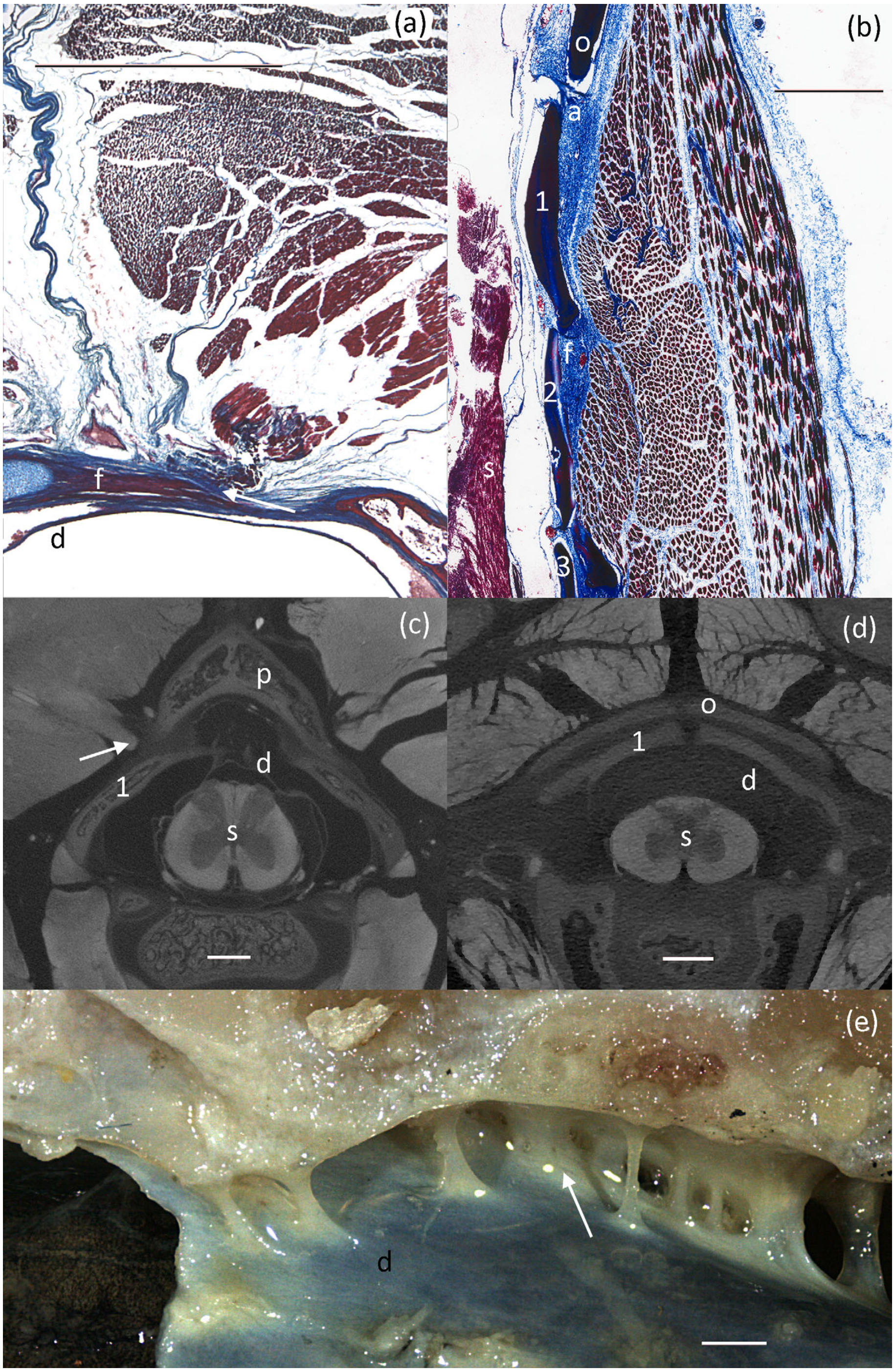

FIGURE 6 Comparison between *Crotalus atrox* and *Alligator mississippiensis*. (a) Transverse section from *A. mississippiensis*. (b) Sagittal section from *C. atrox*. (c) Micro-CT image in the transverse plane from *A. mississippiensis*. (d) Micro-CT image in the transverse plane from *C. atrox*. (e) Sagittal section through the neck region of a sub-adult *A. mississippiensis*. All of the *A. mississippiensis* sections show a myodural bridge (white arrows) made up of muscle fibers deviating toward the spinal cord with tendinous elements passing through the intervertebral joint to contact the dura. No comparable morphology is present in *C. atrox*. 1, C1 vertebra (atlas); 2, C2 vertebra (axis); 3, C3 vertebra; d, dura; f, ligamentum flavum; o, otoccipital; p, proatlas; s, spinal cord. The scale bar in each image is = 1 mm

The approach used for this analysis—complete serial sections in multiple planes and micro-CT analyses—provides more than enough anatomical resolution to document the MDB if one were present. Though this study was framed around the definition of the MDB given by Hack et al. (1995), we examined a much larger anatomical region. As evidenced in Figures 1–4, we looked at all of the “neck” region of the species examined, including all of the suboccipital and axial muscles, ligamentum flavum as well as the atlantooccipital membrane, and the joints between (at least) the skull/C1, C1/C2, and C2/C3.

This “larger” perspective was warranted because following the precise definition provided by Hack et al. (1995) there has been a flurry of descriptions (mainly in humans) of other muscles proposed to also form an MDB. These include rectus capitis posterior major, obliquus capitis inferior, and a number of back muscles by way of the ligamentum nuchae (see Palomeque-del-Cerro et al., 2017 for a review). Biomechanical evidence demonstrates that when the MDB includes prominent tendinous elements spanning between the muscle fibers and the dura, there is functionally relevant force transmission between the muscle and the dura (Venne et al., 2017). No comparable experimental evidence exists for an MDB, which includes only fascial connections but not tendinous elements connecting to the dura. The outer surface of the dura has connective tissue ties to the vertebrae and ligamentum flavum (including epidural, Hoffmann's, and meningovertebral ligaments) as well as connective tissue links at the intervertebral foramina (e.g., Bosscher et al., 2021; Kimmell et al., 2011; Tardieu et al., 2016). As such, the presence of a connective tissue link between the dura and the atlantooccipital membrane (or ligamentum flavum) cannot be taken, in and of itself, as evidence of an MDB.

No evidence of an MDB was found among the snake species examined, though the application of the same morphological criteria identified the MDB in *A. mississippiensis*. Most of the snakes examined for this study had smaller heads than any of the other species from which an MDB has been described, but this does not seem adequate to explain the absence of this morphological complex. We examined the *Ophiophagus* specimen, in part, because the head of this specimen (Figure 6a) was larger than the head of the hatchling *Alligator* specimens. All of the snake species examined in this study were characterized by extensive bony overlap at the skull/C1, C1/C2, and C2/C3 joints (Figure 6a). In all of the snake specimens examined, at the otooccipital/C1 joint (Figure 1), the C1/C2 joint (Figure 2), and the C2/C3 joint (Figure 3), the successive vertebrae were so physically close that they overlapped in all histological sections; that is, there was not a 10 μm gap along the dorsal or dorsolateral surfaces between successive vertebrae. These extensive intervertebral contact areas have been previously described in snakes (Hoffstetter & Gasc, 1969; Jandzik & Bartik, 2004). This close apposition of successive vertebrae is in marked contrast to the condition found in *Alligator* (Figure 6b,c), and would restrict the passageway of tendinous elements from an MDB.

It would be premature, based on the examination of six species, to assert that an MDB was lacking in all snakes. Further comparative work, perhaps involving burrowing snakes (such as *Heterodon* or *Uropeltis*) that have specialized cervical axial musculature (Deufel, 2017), or taxa with differently shaped neural arches (e.g., Ikeda, 2007) may reveal an ophidian MDB. Zheng et al. (2017) postulated that the MDB was a universal feature of mammals; this may prove correct, but to date evidence only exists for a small sampling of mammalian taxa. Furthermore, the mammalian taxa in which MDBs have been studied are all characterized by “normal” ranges of head movement and force application. It would be interesting to see how the MDB was structured in more specialized groups, such as taxa that burrow with their head (e.g., Wake, 1993).

Previous workers have hypothesized that the MDB functions to sense dural tension (e.g., Hallgren et al., 1997). While the dura contains sensory neurons, as does the peridural membrane and other epidural tissue (e.g., Bosscher et al., 2016; Bridge, 1959), there is little functional evidence relating this spinal sensory complex to the MDB. The MDB itself could play a sensory role; if so, the muscle fascicles that contact the dura should have an increased density of spindle organs compared to fascicles from the same muscle that inserts onto the skull (e.g., Hallgren et al., 1997). No evidence of these sensory receptors has yet been reported. Given how posturally dynamic snakes are, particularly arboreal snakes like *Crotaphopeltis* and *Toxicodryas*, and that postural changes in snakes are associated with marked changes in CSF pressure (Young, Greer, & Cramberg, 2021), it is difficult to understand why snakes would lack an MDB sensory system that is present in turtles (Huangfu et al., 2019).

The MDB has been hypothesized to function in stabilizing the dura, preventing dural prolapse or collapse in the cervical region (Hack et al., 1995). In support of this hypothesis, researchers cite reports of dural folds in the cervical region located in close proximity to the MDB (e.g., Ito et al., 2020). Dural folds or pleats in the proximity of the foramen magnum have not been described in all of the species in which an MDB has been reported, nor is it clear that in all species the range of the MDB would be sufficient to prevent dural prolapse or pleating.

Contraction of the MDB would expand the diameter of the dura creating a localized change in subarachnoid volume, and with it, CSF pressure. This was the basis for the hypothesis that the MDB functions as a CSF “pump” (Sui et al., 2013; Zheng et al., 2014) to drive the CSF in the spinal canal. The ability of the MDB to alter CSF pressure has been demonstrated experimentally. Venne et al. (2017) demonstrated that in the human cadaveric material force applied to the MDB was sufficient to displace the cervical dura. Electrical stimulation of the MDB was shown to alter CSF pressure in anesthetized alligators (Young, Adams, et al., 2021; Young et al., 2020) and dogs (Ma et al., 2021). Active movement of the human head (Xu et al., 2016), and passive movement of the dog's head (Ma et al., 2021) have been shown to induce CSF flow. Earlier (Young, Adams, et al., 2021) it was argued that this myodural-based alteration of CSF dynamics is better viewed as “stirring” than a “pump”; the interaction between the MDB and the spinal CSF does not include a one-way valve as would be required in a true pump. In the data reported by Ma et al. (2021), there was no significant difference in the volume of CSF flowing away from, then subsequently toward, the activated MDB.

Herein, we hypothesize that the primary function of the MDB, contracting alone or during displacement of the head, is to create a pulsation of CSF pressure to drive (clear) the CSF from the parenchyma of the CNS and from the subarachnoid space. The MDB is capable of producing transitory CSF pressures greater than those attributed to the cardiac pulsations (Ma et al., 2021; Young, Adams, et al., 2021; Young et al., 2020). As such, the MDB could exert a significant influence on the hydrostatic balance of the CSF. For example, an MDB-induced increase in CSF pressure would impede CSF production at the choroid plexus. It seems more likely that the major influence of the MDB is on CSF clearance or absorption.

The MDB-induced pressure pulsations would drive the CSF across the arachnoid granulations located in the cranial dural sinuses (Proulx, 2021) and along the spinal nerves (e.g., Jagla et al., 2009). Since the exchange between the CSF and the venous vessel is based on differential pressure (e.g., Sakka et al., 2011), a transitory increase in CSF pressure from the MDB would increase CSF loss, and the return to resting CSF pressure would not be associated with an influx of CSF. The myodural pressure pulsation would force more subarachnoid CSF both through the cribriform plate (e.g., Norwood et al., 2019), and into any lymphatic vessels draining the dura (e.g. Ahn et al., 2019; Bradbury et al., 1981). As with the subarachnoid granulations, this movement of CSF would be unidirectional. Weller et al. (2009) detailed the challenge of passing interstitial fluid along with the perivascular space against the flow of blood; the myodural pulsations which are temporally independent of, and greater in magnitude than, the arterial pulsations, could generate some perivascular flow of interstitial fluid. Since the CSF pressure pulsations caused by the MDB are larger than those caused by the cardiac cycle, activation of the MDB may cause CSF loss along different pathways (Vinje et al., 2020). This hypothesis could be readily tested by looking for differential CSF marker clearance during rest, passive head movements, and active stimulation of the MDB.

Since no evidence of an MDB was found in the snakes examined in this study, would snakes have a lower rate of CSF clearance? Possibly, but the MDB is not the only potential source of transitory CSF pulsations. It was recently shown (Young, Greer, & Cramberg, 2021) that undulatory vertebral displacement of the snake's body produces pressure pulsations in the CSF similar to those produced by the MDB. These locomotor-linked CSF pulsations appear to arise from impulses acting on the CSF, but could be manifestations of spinal cord (Rade et al., 2016) or dural (Young, Greer, & Cramberg, 2021) displacement. In either case, they appear to be the "trunk" equivalent of the effect of passive or active head displacement on the cranial CSF (Ma et al., 2021; Xu et al., 2016). Snakes may routinely utilize more vertebral deflection than any other vertebrate group; as such, the abundance of "trunk" pulsations may have alleviated the need for the MDB in these vertebrates.

This hypothesis, that vertebral deflection could explain the absence of the MDB, could be readily tested through a comparative study of the suboccipital region in lizards. The results of the present study suggest that elongate limbless or nearly limbless lizards, which locomote almost exclusively through axial deflection, would have a poorly developed MDB. In contrast, lizards that utilize appendicular propulsion with little axial deflection, are predicted to have greater development of the MDB.

5 | CONCLUSION

The MDB was originally described as muscle fibers of the rectus capitis posterior inferior which deviated toward the spinal cord, had tendinous elements which passed through the atlantooccipital membrane, and directly attached to the cervical dura mater. Applying this definition to a group of African Colubrine snakes, revealed no evidence for an MDB. The defining criteria for the MDB were expanded to include: (1) any skeletal muscle; (2) any of the "cervical" intervertebral joints; (3) any collagen fibers coursing from the muscle to the cervical dura. Additional species, representing two other distantly related snake lineages, were also examined; still no evidence for an MDB was found. The same criteria were applied to *A. mississippiensis*, which had an evident MDB. Snakes are the only amniotes that appear to lack an MDB. It is hypothesized that the close apposition of the neural arches in snakes examined may preclude muscle tendons passing through the dorsal portion of the intervertebral joint. Herein, it is proposed that the MDB creates episodic pulses of CSF pressure, which function to clear the CSF from the subarachnoid space and the interstitial tissue.

ACKNOWLEDGMENTS

The authors are indebted to the imaging department of the Northeastern Regional Medical Center (Kirksville, MO) for their assistance with the CT images. We thank J. Adams, R. Elsey, and P. Kondrashov for their support, and K.-A. Mardal for his insightful comments on an early version of this manuscript.

CONFLICT OF INTEREST

The authors declare no conflicts of interests.

AUTHOR CONTRIBUTIONS

Bryson Grondel: Formal analysis, investigation, validation, visualization, writing-review & editing. **Skye Greer**: Formal analysis, investigation, validation, visualization, writing-review & editing. **Michael Cramberg**: Formal analysis, investigation, methodology, resources, supervision, validation, visualization, writing-review & editing. **Bruce A. Young**: Conceptualization, data curation, formal analysis, funding acquisition, investigation, methodology, project administration, resources, supervision, validation, visualization, writing-original draft preparation, writing-review & editing.

PEER REVIEW

The peer review history for this article is available at https://publons.com/publon/10.1002/jmor.21431.

DATA AVAILABILITY STATEMENT

The anatomical material generated during this study are available through requests to the corresponding author.

ORCID

Bruce A. Young https://orcid.org/0000-0002-0988-7731

REFERENCES

Ahn, J. H., Cho, H., Kim, J. H., Kim, S. H., Ham, J. S., Park, I., Suh, S. H., Hong, S. P., Song, J.-H., Hong, Y.-K., Jeong, Y., Park, S.-H., & Koh, G. Y. (2019). Meningeal lymphatic vessels at the skull base drain cerebrospinal fluid. *Nature*, *572*, 62–66.

Barfuss, D., & Dantzler, W. (1976). Glucose transport in isolated perfused proximal tubules of snake kidney. *American Journal of Physiology*, *231*, 1716–1728.

Bordoni, B., & Myers, T. (2021). A review of the theoretical fascial models: Biotensegrity, fascintegrity, and myofascial chains. *Cureus*, *12*, e7092. https://doi.org/10.7759/cureus.7092

Bosscher, H. A., Grazdanov, P. N., Warraich, I. I., MacDonald, C. C., & Day, M. R. (2021). The anatomy of the peridural membrane of the human spine. *Anatomical Record*, *304*, 677–691.

Bosscher, H. A., Heavner, J. E., Grozdanov, P., Warraich, I. A., Wachtel, M. S., & Dertien, J. (2016). The peridural membrane of the human spine is well innervated. *Anatomical Record*, *299*, 484–491.

Bradbury, M. W., Cserr, H. F., & Westrop, R. J. (1981). Drainage of cerebral interstitial fluid into deep cervical lymph of the rabbit. *American Journal of Physiology*, *240*, F329–F336.

Bridge, C. J. (1959). Innervation of spinal meninges and epidural structures. *Anatomical Record*, *133*, 553–561.

Broadley, D. G. (1983). *FitzSimons' snakes of southern Africa*. Delta Books.

Chen, C., Yu, S.-B., Chi, Y.-Y., Tan, G.-Y., Yan, B.-C., Zheng, N., & Sui, H.-J. (2021). Existence and features of the myodural bridge in *Gentoo penguins*: A morphological study. *PLoS One*, *16*, e0244774. https://doi.org/10.1371/journal.pone.0244774

Deufel, A. (2017). Burrowing with a kinetic snout in a snake (Elapidae: *Aspidelaps scutatus*). *Journal of Morphology*, *278*, 1706–1715.

Dou, Y. R., Zheng, N., Gong, J., Tang, W., Okoye, C. S., Zhang, Y., Chen, Y.-X., Pi, S.-Y., Qu, L.-C., Yu, S.-B., & Sui, H.-J. (2019). Existence and features of the myodural bridge in *Gallus domesticus*: Indication of its important physiological function. *Anatomical Science International*, *94*, 184–191. https://doi.org/10.1007/s12565-018-00470-2

Dreha-Kulaczewski, S., Joseph, A., Merboldt, K.-D., Ludwig, H.-C., Gartner, J., & Frahm, J. (2015). Inspiration is the major regulator of human CSF flow. *Journal of Neuroscience*, *35*, 2485–2491.

Elbrond, V. S., & Schultz, R. M. (2019). Equine myodural bridges - an anatomical, integrative and functional description of myodural bridges along the spine of horses: Special focus on the atlanto-occipital and alanto-axial regions. *Medical Research Archives*, *7*, 1–20.

Enix, D. E., Scali, F., & Pontell, M. E. (2014). The cervical myodural bridge, a review of literature and clinical implications. *The Journal of the Canadian Chiropractic Association*, *58*, 184–192.

Figueroa, A., McKelvy, A. D., Grismer, L. L., Bell, C. D., & Lailvaux, S. P. (2016). A species-level phylogeny of extant snakes with description of a new Colubrid subfamily and genus. *PLoS One*, *11*, e0161070. https://doi.org/10.1371/journal.pone.0161070

Glaudas, X., Glennon, K. L., Martins, M., Luiselli, L., Fearn, S., Trembath, D. F., Jelic, D., & Alexander, G. J. (2019). Foraging mode, relative prey size and diet breadth: A phylogenetically explicit analysis of snake feeding ecology. *Journal of Animal Ecology*, *88*, 757–767.

Hack, G. D., Kortizer, R. T., & Robinson, W. L. (1995). Anatomic relation between the rectus capitis posterior minor muscle and the dura mater. *Spine*, *20*, 2484–2486.

Hallgren, R. C., Hack, G. D., & Lipton, J. A. (1997). Clinical implications of a cervical myodural bridge. *AAOJ*, *7*, 30–34.

Hoffstetter, R., & Gasc, J.-P. (1969). Vertebrae and ribs of modern reptiles. In C. Gans, A. D'A Bellairs, & T. S. Parsons (Eds.), *Biology of the Reptilia* (Vol. 1, pp. 201–310). Academic Press.

Huangfu, Z., Zhang, X., Sui, J.-Y., Zhao, Q.-Q., Yuan, X.-Y., Li, C., Dou, Y.-R., Tang, W., Du, M.-L., Zheng, N., Chi, Y.-Y., Yu, S.-B., & Sui, H.-J. (2019). Existencia del Puente Miodural en *Trachemys scripta elegans*: indicacion de su importante funcion fisiologica. *International Journal of Morphology*, *37*, 1353–1360.

Ikeda, T. (2007). A comparative morphological study of the vertebrae of snakes occurring in Japan and adjacent regions. *Current Herpetology*, *26*, 13–34.

Ito, K., Yamada, M., Horiuchi, T., & Hongo, K. (2020). Microanatomy of the dura mater at the craniovertebral junction and spinal region for safe and effective surgical treatment. *Journal of Neurosurgery: Spine SPI*, *33*, 165–171.

Jagla, G., Walocha, J., Rajda, K., Dobrogowski, J., & Wordliczek, J. (2009). Anatomical aspects of epidural and spinal analgesia. *Advances in Palliative Medicine*, *8*, 135–146.

Jandzik, D., & Bartik, I. (2004). Differences in morphology of the atlas-axis complex in *Natrix natrix* and *N. tessellata* (Serpentes: Colubridae). *Biologica Bratislava*, *15*, 219–229.

Kimmell, K. T., Dayoub, H., Shakir, H., & Sincott, E. H. (2011). Spinal dural attachments to the vertebral column: An anatomic report and review of the literature. *Surgical Neurology International*, *2*, 97. https://doi.org/10.4103/2152-7806.82990

Kondrashova, T., Blanchard, J., Knoche, L., Potter, J., & Young, B. A. (2020). Intracranial pressure in the American alligator (*Alligator mississippiensis*): Reptilian meninges and orthostatic gradients. *Journal of Comparative Physiology A*, *206*, 45–54.

Lai, H. X., Zhang, J. F., Song, T. W., Liu, B., Tang, W., Sun, S. Z., Qin, T., Yun, Z. F., Zhu, S. J., Yu, S. B., & Sui, H. J. (2020). Development of myodural bridge located within the atlanto-occipital interspace of rats. *Anatomical Record*, *304*, 1541–1550.

Liu, P., Li, C., Zheng, N., Xu, Q., Yu, S.-B., & Sui, H.-J. (2017). The myodural bridge existing in the *Nephocaena phocaenoides*. *PLoS One*, *12*, e0173630. https://doi.org/10.1371/journal.pone.0173630

Liu, P., Li, C., Zheng, N., Yuan, X., Zhou, Y., Chun, P., Chi, Y., Gilmore, C., Yu, S., & Sui, H. (2018). The myodural bridges' existence in the sperm whale. *PLoS One*, *13*, e0200260. https://doi.org/10.1371/journal.pone.0200260

Ma, Y., Tang, W., Gong, D.-Z., Li, X.-Y., Zhang, J.-H., Sun, J.-H., Wang, B., Zhang, Y., Chen, Y.-X., Zhang, Z.-H., Zheng, N., Okoye, C. S., Chi, Y.-Y., Wu, C.-W., Yu, S.-B., & Sui, H.-J. (2021). The morphology, biomechanics, and physiological function of the suboccipital myodural connections. *Scientific Reports*, *11*, 8064. https://doi.org/10.1038/s41598-021-86934-4

Norwood, J. N., Zhang, Q., Card, D., Craine, A., Ryan, T. M., & Drew, P. J. (2019). Anatomical basis and physiological role of cerebrospinal fluid transport through the murine cribriform plate. *eLife*, *8*, e44278. https://doi.org/10.7554/eLife.44278

Okoye, C. S., Zheng, N., Yu, S. B., & Sui, H. J. (2018). The myodural bridge in the common rock pigeon (*Columbia livia*): Morphology and possible physiological implications. *Journal of Morphology*, *279*, 1524–1531.

Palomeque-del-Cerro, L. T., Arráez-Aybar, L. A., Rodríguez-Blanco, C., Guzmán-García, R., Menendez-Aparicio, M., & Oliva-Pascual-Vaca, Á. (2017). A systematic review of the soft-tissue connections between neck muscles and Dura mater. *Spine*, *42*, 49–54. https://doi.org/10.1097/BRS.0000000000001655

Proulx, S. T. (2021). Cerebrospinal fluid outflow: A review of the historical and contemporary evidence for arachnoid villi, perineural routes, and dural lymphatics. *Cellular and Molecular Life Sciences*, *78*, 2429–2457. https://doi.org/10.1007/s00018-020-03706-5.PMC8004496

Rade, M., Könönen, M., Marttila, J., Shacklock, M., Vanninen, R., Kankaanpää, M., & Airaksinen, O. (2016). In vivo MRI measurement of spinal cord displacement in the thoracolumbar region of asymptomatic subjects with unilateral and sham straight leg raise tests. *PLoS One*, *11*, e0155927. https://doi.org/10.1371/journal.pone.0155927

Sakka, L., Coll, G., & Chazal, J. (2011). Anatomy and physiology of the cerebrospinal fluid. *European Annals of Otorhinolaryngology, Head and Neck Diseases*, *128*, 309–316.

Spawls, S., & Branch, B. (1995). *The dangerous snakes of Africa*. Ralph Curtis Publishing.

Sui, H. J., Yu, S. B., Yuan, X. Y., Gao, H. B., Xu, Q., Li, Y. F., & Chi, Y. Y. (2013). Anatomical study on the connections between the suboccipital structures and the spinal dura mater. *Chinese Journal of Clinical Anatomy*, *31*, 489–490.

Tardieu, G. G., Fisahn, C., Loukas, M., Moisi, M., Chapman, J., Oskouian, R. J., & Tubbs, R. S. (2016). The epidural ligaments of Hofmann: A comprehensive review of the literature. *Cureus*, *8*, e779. https://doi.org/10.7759/cureus.779

Venne, G., Rasquinha, B. J., Kunz, M., & Ellis, R. E. (2017). Rectus capitis posterior minor. *Spine*, *42*, 466–473. https://doi.org/10.1097/BRS.000000000000186

Vinje, V., Eklund, A., Mardal, K.-A., Rognes, M. E., & Stoverud, K.-H. (2020). Intracranial pressure elevation alters CSF clearance pathways. *Fluids and Barriers of the CNS*, *17*, 1–19.

Wake, M. (1993). The skull as a locomotor organ. In J. Hanken & B. K. Hall (Eds.), *The skull, functional and evolutionary mechanisms* (Vol. 3, pp. 197–240). University of Chicago Press.

Weller, R. O., Djuanda, E., Yow, H.-Y., & Carare, R. O. (2009). Lymphatic drainage of the brain and the pathophysiology of neurological disease. *Acta Neuropathology*, *117*, 1–14.

Wiens, J. J., Hutter, C. R., Mulcahy, D. G., Noonan, B. P., Townsend, T. M., Sites, J. W., Jr., & Reeder, T. W. (2012). Resolving the phylogeny of lizards and snakes (Squamata) with extensive sampling of genes and species. *Biology Letters*, *8*, 1043–1046.

Xu, Q., Yu, S. B., Zheng, N., Yuan, X. Y., Chi, Y. Y., Liu, C., Wang, X.-M., Lin, X.-T., & Sui, H. J. (2016). Head movement, an important contributor to human cerebrospinal fluid circulation. *Scientific Reports*, *6*, 31787.

Young, B. A., Adams, J., Beary, J. M., Mardal, K.-A., Schneider, R., & Kondrashova, T. (2020). The myodural bridge of the American alligator (*Alligator mississippiensis*) alters CSF flow. *Journal of Experimental Biology*, *223*, jeb230896. https://doi.org/10.1242/jeb.230896

Young, B. A., Adams, J., Beary, J. M., Mardal, K.-A., Schneider, R., & Kondrashova, T. (2021). Variations in the cerebrospinal fluid dynamics of the American alligator (*Alligator mississippiensis*). *Fluids Barriers CNS*, *18*, 11. https://doi.org/10.1186/s12987-021-00248-1

Young, B. A., Greer, S., & Cramberg, M. (2021). Slithering CSF: Cerebrospinal fluid dynamics in the stationary and moving viper boa, *Candoia aspera*. *Biology*, *10*, 672. https://doi.org/10.3390/biology10070672

Zhang, J. H., Tang, W., Zhang, Z. X., Luan, B. Y., Yu, S. B., & Sui, H. J. (2016). Connection of the posterior occipital muscle and dura mater of the *Siamese crocodile*. *Anatomical Record*, *299*, 1402–1408.

Zhang, Z.-H., Zhang, Y., Sun, J.-X., Ding, S.-W., Ma, G.-J., Chi, Y.-Y., Yu, S.-B., Zheng, N., & Sui, H.-J. (2020). Scanning electron microscopy of myodural bridge in dog. *Acta Anatomica Sinica*, *51*, 929–933.

Zheng, N., Yuan, X. Y., Chi, Y. Y., Liu, P., Wang, B., Sui, J.-Y., Han, S.-H., Yu, S.-B., & Sui, H.-J. (2017). The universal existence of myodural bridge in mammals: An indication of a necessary function. *Scientific Reports*, *7*, 8248. https://doi.org/10.1038/s41598-017-06863-z

Zheng, N., Yuan, X. Y., Li, Y. F., Chi, Y. Y., Gao, H. B., Zhao, X., Yu, S.-B., Sui, H.-J., & Sharkey, J. (2014). Definition of the to be named ligament and vertebrodural ligament and their possible effects on the circulation of CSF. *PLoS One*, *9*, e103451.

How to cite this article: Grondel, B., Cramberg, M., Greer, S., & Young, B. A. (2021). The morphology of the suboccipital region in snakes, and the anatomical and functional diversity of the myodural bridge. *Journal of Morphology*, *283*(1), 123–133. https://doi.org/10.1002/jmor.21431